Research article Available online www.ijsrr.org ISSN: 2279–0543

International Journal of Scientific Research and Reviews

# Quantum mechanical studies on spectral and electronic characteristics of Pioglitazone a potent DPP – 4 inhibitor

**B. Vijayakumar[a*], V.Sathyanarayanamoorthi[b], V.Kannappan[c], P.Nareshkumar[d]**

[a] Department of Physics, Research & Development Centre, Bharathiar University, Coimbatore 641 046, India
[b] Department of Physics, PSG College of Arts and Science, Coimbatore 641 014,India
[c] Department of Chemistry, Presidency College, Chennai 600 005,India
[d] Department of Physics, SNS College of Technology, Coimbatore 641 035,India

## ABSTRACT

In this present work, Quantum mechanical studies are carried out on a new generation drug Pioglitazone (PGZE) to understand the spectral and electronic characteristics of the molecule. The optimized molecular geometry, atomic charges, dipole moment, rotational constants and several thermodynamic parameters of the molecule in the ground state were calculated using ab initio Hartree–Fock (HF) and Density Functional B3LYP methods (DFT) with 6-311++G(d,p) basis sets. The theoretical scaled vibrational frequencies have been assigned and they agreed satisfactorily with experimental FT-IR and Raman frequencies. The theoretical maximum wavelengths of absorption of are calculated in water, ethanol, and methanol by the TD-DFT method and these values are compared with experimentally determined $\lambda_{max}$ values. The spectral and Natural bonds orbital (NBO) analysis in conjunction with spectral data established the presence of intramolecular interactions such as delocalisation, hyperconjugative and stereoelectronic effect. The energy gap of the molecule was found using HOMO and LUMO calculation, hence the less band gap, which seems to be more stable. Computed values of Mulliken charges of are reported.

**KEYWORDS**: Pioglitazone; DFT study; FT-IR, FT-Raman, and electronic spectra; NBO and NLO analysis; thermodynamic properties

***Correspondence author**

## B. Vijayakumar

Department of Physics,

Research & Development Centre,

Bharathiar University, Coimbatore 641 046, India

Email: vijay10678@yahoo.com Mobile: 9994346411

# 1. INTRODUCTION

Pioglitazone or [(±)-5-[[4-[2-(5-ethyl-2-pyridinyl)ethoxy]phenyl]methyl]-2,4-]thiazolidinedione monohydrochloride is a different pharmacological action than the sulfonylureas, metformin, or the α-glucosidase inhibitors. The molecule contains one asymmetric carbon, and the compound is synthesized and used as the racemic mixture. pioglitazone as monotherapy or in combination with other oral antidiabetic drugs or insulin has demonstrated to effectively improve blood glucose levels, long-term glucose control, and the lipid profile. The drug is well tolerated and has an acceptable side effect profile. Because of its additional microvascular and macrovascular effects, pioglitazone is an attractive and effective treatment option for the management of Type 2 diabetes mellitus[1]. Pioglitazone which is approximately 10 times less potent than rosiglitazone, enhances the mRNA expression of the proatherogenic factors and adipophilin[2]. The literature survey reveals that chromatographic methods are reported for simultaneous estimation of pioglitazone and its metabolites in human plasma, human serum, and urine [3, 4, 5] .The quantum mechanical studies carry out of molecule to understand the structural conformation of this compound and geometrical parameters are reported for the ground state. The energy gap is computed using the Gaussian 09W program. The NBO analysis to get an evidence of redistribution electron density (ED) in various bonding, anti-bonding orbital's and E(2) energies are calculated by the stability of due to various intra-molecular interactions. HOMO- LUMO analysis has been used to establish charge transfer within the molecule. Mulliken population analysis of is also carried out.

# 2. MATERIALS AND METHODS

## *2.1EXPERIMENTAL*

The drug pioglitazone with a purity of 99.5% is purchased from Sigma Aldrich chemical suppliers (India). Spectra were recorded for with the sample as received. FT-IR spectrum was recorded in the wavenumber region 400–4000 $cm^{-1}$ on a PERKIN ELMER spectrophotometer equipped with mercury, cadmium and tellurium detector in a KBr pellet technique with a resolution of 1.0 $cm^{-1}$. The FT-Raman spectrum was obtained for the compound in the wavenumber region 50–4000 $cm^{-1}$ on a BRUKER RFS27 spectrophotometer equipped with Raman module accessory operating at 1.5 W power with Nd:YAG laser and the excitation wavelength was 1064 nm. The spectra were recorded in the Regional Sophisticated Centre, Indian Institute of Technology, Chennai-600036. India. UV-vis. spectra were recorded on a Shimadzu UV – 1650 model spectrophotometer with quartz cell of 1 cm optical path length. The baseline correction was done with the solvents (water, ethanol, and methanol). The absorption spectra were recorded in the wavelength region of 200 – 600nm at a scanning rate of 0.2 nm/s and a slit width of 1cm.

### 2.2 Computational details

The quantum mechanical computations were performed on by using Gaussian 09 program package [6] at the HF and B3LYP [7, 8] levels with 6-311++G (d, p) basis set to obtain geometry optimization. Molecular vibrations and their displacement vectors were obtained using Gauss View interface program [9]. A uniform scaling factor of 0.9533 and 0.9615 was adopted for vibrational frequencies obtained from HF/ 6-311++G (d, p) and B3LYP/6-311++G (d, p) method. The computed Raman activities ($S_i$) were converted to relative Raman intensities ($I_i$) using the equation [1] which was derived from the basic theory of Raman scattering[10, 11].

$$I_i = \frac{f(\nu_o - \nu_i)^4 S_i}{\nu_i \left[1 - \exp\left[\frac{-hc\nu_i}{K_b T}\right]\right]} \qquad \ldots\ldots\ldots (1)$$

Where, $\nu_o$ is the exciting frequency (in $cm^{-1}$ ), $\nu_i$ is the vibrational wavenumber of the $i^{th}$ normal mode, h, c, and k are universal constants and *f* is suitably chosen common scaling factor for all the peak intensities. The electronic transitions, vertical excitation energies, absorbance and oscillator strengths of the PGZE molecule are calculated with the TD-DFT/6-311++G(d,p) method. The Molecular Orbital calculations such as NBO and HOMO–LUMO are performed on DDT-4 by both HF and DFT methods. These results have also been used to calculate the thermodynamic properties such as heat capacity, entropy, and enthalpy. Mulliken charges and molecular properties of PGZE (dipole moment, mean polarizability and first static hyperpolarizability) are calculated using on the finite field approach.

## 3. RESULTS AND DISCUSSION

### 3.1 Molecular geometric parameters

Fig.1. Shows the numbering system adopted in the molecular structure of PGZE. The HF and B3LYP methods with 6-311++G(d,p) basis set calculate the most optimized structural parameters and these properties are presented in Table 1. The geometrical parameters of bond lengths and bond angles were obtained from HF and B3LYP method. It may be pointed out that the bond lengths obtained by both HF and B3LYP methods are comparable and the bond lengths obtained by the B3LYP method are slightly longer than those calculated by HF method. In this calculation, the amino N-H bond has a length of about 1 **Å** for both HF and DFT method**.** It is also found that all the six C-C bonds of the benzene ring are not of equal length. It is observed that the C17–C18–C19 bond angles are slightly greater than 120° while C18–C19–C20 angle is less than 120°. The C-N-C bond angles are larger than the N-C-C bond angles[12]. Gundersen and Rankin have determined the C-N-C (110.7°) and N-C-C (110.5°) bond angles in piperidine by electron diffraction technique[13]. In the

work, the bond angles of C2–N3–C4 (120.65°), N3–C4–C5 (112.8°) and C18–N23–C22 (119.04°) by B3LYP/6-311++G(d,p) method. Thus, in the present work, we have focused on the most stable form of a molecule to clarify the molecular structure and assignments of vibrational spectra by B3LYP/6-311++G(d,p) method. In the thiazolidinedione ring system bond length N3–C4 is 1.3863**Å** and C2–N3bond is 1.3932 **Å**. Both are the almost equal bond length. This may be attributed to the heteroatom effect of N3 and S1 the adjacent benzene ring. S1–C2–N3bond angle is about 109°. However, N3–C4–O7and S1–C5–C8 bond angles are much larger. Thus, the bond lengths and bond angles in the thiazolidinedione heterocyclic system are influenced by substitution. The bond length for S1–C2, S1–C5, C5–C8, and C24–C25 are found to be 1.8602, 1.9174, 1.5419 and 1.5437**Å** respectively. Many researchers have explained the changes in the bond lengths or frequencies are due to the substituent and significance charge distribution on the carbon atom of the aromatic ring compound. The substituent may play a very important role in the structural and electronic properties of the molecules. For the title molecule, the bond length of the group (C-N) is predicted to be 1.3932 **Å** and it shows good agreement with the experimental data [14] of 1.145 **Å**. With the electron donating substituents on the benzene ring, the symmetry of the ring is distorted, yielding ring angles smaller than 120° at the point of substitution and slightly larger than 120° at the two ortho positions[15]. More distortion in bond parameters is observed in the hetero ring than the benzene ring. The variation in bond angle depends on the electronegativity of the central atom. If the electronegativity of the central atom decreases, the bond angle decreases. Thus the bond angle C2–S1–C5 very less (90.97°) than the bond angle S1–C5–C4is (106.50°) is the reason for the high electronegativity of nitrogen.

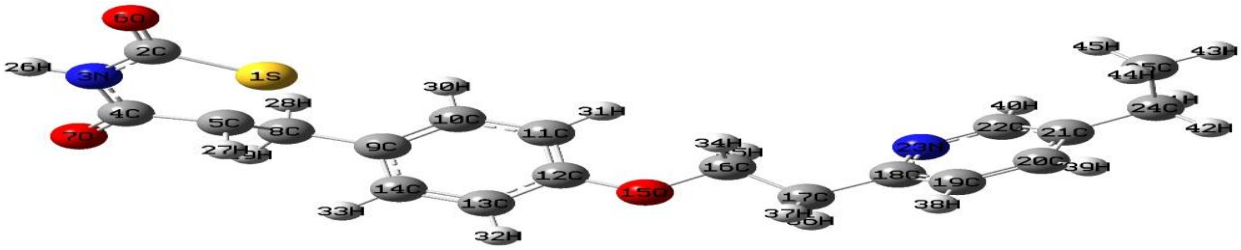


**Fig.1: Optimized molecular structure of PGZE**

**Table 1: Optimized Selected Bond lengths and bond angles of PGZE molecule obtained by HF/6-311G++ (d,p) and B3LYP/6-311G++(d,p) methods**

| Bond length | HF | B3LYP | Bond angle | HF | B3LYP | Bond angle | HF | B3LYP |
|---|---|---|---|---|---|---|---|---|
| S1–C2 | 1.8264 | 1.8602 | C2–S1–C5 | 91.35 | 90.97 | C16–C17–C18 | 112.57 | 112.57 |
| S1–C5 | 1.8919 | 1.9174 | S1–C2–N3 | 109.52 | 109.04 | C16–C17–H36 | 108.23 | 107.81 |
| C2–N3 | 1.3741 | 1.3932 | S1–C2–O6 | 125.66 | 125.69 | C16–C17–H37 | 108.86 | 109.31 |
| C2–O6 | 1.2012 | 1.2225 | N3–C2–O6 | 124.8 | 125.26 | C18–C17–H36 | 109.67 | 109.68 |
| N3–C4 | 1.3703 | 1.3863 | C2–N3–C4 | 120.11 | 120.65 | C18–C17–H37 | 110.25 | 110.35 |
| N3–H26 | 0.9933 | 1.0103 | C2–N3–H26 | 119.5 | 119.21 | H36–C17–H37 | 107.05 | 106.90 |
| C4–C5 | 1.5113 | 1.5212 | C4–N3–H26 | 120.37 | 120.12 | C17–C18–N23 | 117.12 | 116.79 |
| C4–O7 | 1.2129 | 1.2367 | N3–C4–C5 | 113.09 | 112.80 | C19–C18–N23 | 120.47 | 120.88 |
| C5–C8 | 1.5341 | 1.5419 | N3–C4–O7 | 123.26 | 123.56 | C18–C19–C20 | 119.36 | 119.50 |
| C5–H27 | 1.0757 | 1.0882 | C5–C4–O7 | 123.64 | 123.62 | C18–C19–H38 | 120.07 | 119.92 |
| C8–C9 | 1.5110 | 1.5137 | S1–C5–C4 | 105.87 | 106.50 | C20–C19–H38 | 120.56 | 120.57 |
| C8–H28 | 1.0808 | 1.0915 | S1–C5–C8 | 113.27 | 113.08 | C19–C20–C21 | 120.19 | 120.07 |
| C8–H29 | 1.0815 | 1.0933 | S1–C5–H27 | 106.58 | 106.16 | C19–C20–H39 | 119.82 | 120.08 |
| C9–C10 | 1.3853 | 1.3991 | C4–C5–C8 | 112.09 | 112.02 | C21–C20–H39 | 119.98 | 119.92 |
| C9–C14 | 1.3972 | 1.4074 | C4–C5–H27 | 108.09 | 108.46 | C20–C21–C22 | 116.46 | 116.64 |
| C10– C11 | 1.3912 | 1.3996 | C8–C5–H27 | 110.58 | 110.29 | C20–C21–C24 | 122.06 | 121.99 |
| C10– H30 | 1.0711 | 1.0824 | C5–C8–C9 | 113.43 | 113.71 | C22–C21–C24 | 121.46 | 121.34 |
| C11– C12 | 1.3835 | 1.3980 | C5–C8–H28 | 108.93 | 108.78 | C21–C22–N23 | 123.49 | 123.84 |
| C11–H31 | 1.0680 | 1.0794 | C5–C8–H29 | 106.81 | 106.30 | C21–C22–H40 | 120.67 | 120.48 |
| C12–C13 | 1.3908 | 1.4017 | C9–C8–H28 | 110.31 | 110.53 | N23–C22–H40 | 115.83 | 115.66 |
| C12–O15 | 1.3706 | 1.3907 | C9–C8–H29 | 110.11 | 110.22 | C18–N23–C22 | 120.01 | 119.04 |
| C13–C14 | 1.3783 | 1.3895 | H28–C8–H29 | 106.97 | 106.98 | C21–C24–C25 | 113.14 | 113.07 |
| C13–H32 | 1.0688 | 1.0803 | C8–C9–C10 | 121.59 | 121.48 | C21–C24–H41 | 109.31 | 109.33 |
| C14–H33 | 1.0725 | 1.0836 | C8–C9–C14 | 120.46 | 120.44 | C21–C24–H42 | 109.35 | 109.45 |
| O15–C16 | 1.4356 | 1.4628 | C10–C9–C14 | 117.91 | 118.06 | C25–C24–H41 | 109.18 | 109.16 |
| C16–C17 | 1.5176 | 1.5243 | C9–C10–C11 | 121.50 | 121.45 | C25–C24–H42 | 109.25 | 109.20 |
| C16–H34 | 1.0821 | 1.0937 | C9–C10–H30 | 119.77 | 119.60 | H41–C24–H42 | 106.34 | 106.37 |
| C16–C35 | 1.0774 | 1.0893 | C11–C10–H30 | 118.71 | 118.94 | C24–C25–H43 | 110.72 | 110.77 |
| C17–C18 | 1.5048 | 1.5105 | C10–C11–C12 | 119.55 | 119.46 | C24–C25–H44 | 111.08 | 111.10 |
| C17–H36 | 1.0822 | 1.0939 | C10–C11–H31 | 119.35 | 119.48 | C24–C25–H45 | 110.72 | 110.95 |
| C17–H37 | 1.0803 | 1.0909 | C12–C11–H31 | 121.09 | 121.04 | H43–C25–H44 | 108.03 | 108.03 |
| C18–C19 | 1.3890 | 1.4004 | C11–C12–C15 | 119.81 | 119.91 | H43–C25–H45 | 108.11 | 108.11 |
| C18–N23 | 1.3351 | 1.3556 | C11–C12–O15 | 124.25 | 124.50 | H44–C25–H45 | 107.79 | 107.73 |
| C19–C20 | 1.3841 | 1.3942 | C13–C12–O15 | 115.92 | 115.58 | | | |
| C19–H38 | 1.0698 | 1.0817 | C12–C13–C14 | 119.96 | 119.91 | | | |
| C20–C21 | 1.3906 | 1.4020 | C12–C13–H32 | 118.47 | 118.44 | | | |
| C20–H39 | 1.0720 | 1.0832 | C14–C13–H32 | 121.55 | 121.63 | | | |
| C21–C22 | 1.3880 | 1.4005 | C9–C14–C13 | 121.25 | 121.18 | | | |
| C21–C24 | 1.5102 | 1.5132 | C9–C14–H33 | 119.68 | 119.63 | | | |
| C22–N23 | 1.3308 | 1.3482 | C13–C14–H33 | 119.06 | 119.18 | | | |
| C22–H40 | 1.0705 | 1.0833 | C12–O15–C16 | 121.69 | 119.5 | | | |
| C24–C25 | 1.5354 | 1.5437 | O15–C16–C17 | 106.31 | 106.1 | | | |
| C24–H41 | 1.0826 | 1.0931 | O15–C16–H34 | 109.59 | 109.52 | | | |
| C24–H42 | 1.0831 | 1.0936 | O15–C16–H35 | 110.34 | 110.6 | | | |
| C25–H43 | 1.0825 | 1.0917 | C17–C16–H34 | 110.96 | 111.19 | | | |
| C25–H44 | 1.0824 | 1.0918 | C17–C16–H35 | 110.62 | 110.27 | | | |
| C25–H45 | 1.0821 | 1.0915 | H34–C16–H35 | 108.98 | 109.05 | | | |

### *3.2 Vibrational spectral analysis of PGZE*

FT-IR and FT-Raman spectra of PGZE are recorded in the solid phase, incorporated in KBr pellet. The computed frequency values along with the experimental values are given in Table 2. It is to be noted that the theoretical frequency calculation is done on the gaseous phase of the molecule using HF and B3LYP methods with 6-311++G (d,p) basis set. PGZE molecule consists of 45 atoms and 129 normal vibrational modes are expected as PGZE belongs to C1 point group symmetry. The recorded FT-IR and Raman spectra of PGZE are depicted in Fig.2.

PGZE molecule possesses one methyl group attached to the C24 carbon atom. The $CH_3$ group is basically associated with nine fundamentals[16]. In the present case, the asymmetric methyl stretching bands are observed at 3210 $cm^{-1}$ in FT-IR and FT-Raman spectra values are good and equal. The calculated wavelength by B3LYP/6-311++G(d,p) agrees with the observed frequency. $CH_3$ group was reported at Symmetric and asymmetric deformation vibrations [17] in two regions, namely, 1380–1370 $cm^{-1}$ and 1470–1440 $cm^{-1}$. The stretching modes are observed at 1444 $cm^{-1}$ in B3LYP/6-311G++ (d,p) (modes 92) and experimental value in FT-IR is 1436 $cm^{-1}$ the computed value shows good agreement. Methyl scissoring mode generally appears as a weak, moderate or sometimes strong band in the region 1050 ± 30 $cm^{-1}$ and 975 ± 45 $cm^{-1}$ [18]. This is observed at 1544 and 1550 $cm^{-1}$ in B3LYP/6-311G++G (d,p). $CH_3$ wagging is observed by computed value is 1406 $cm^{-1}$. The deviation ($\Delta\nu$) of this methyl band is 402 $cm^{-1}$. The methyl rocking and torsion modes are assigned at 127 $cm^{-1}$,228 $cm^{-1}$ and 249 $cm^{-1}$ since $CH_3$ in the plane and out of plane bending vibrations are assigned within the characteristic region.

The carbon – carbon stretching modes of the phenyl group are expected in the range from 1650 to 1200 $cm^{-1}$. The actual position of these modes is determined not so much by the nature of the substituent [19]. In this study, the C–C stretching vibration is found at 1263 $cm^{-1}$ to 1280 $cm^{-1}$ by the calculated method. The C–N stretching frequency falls in a complicated region of the vibrational spectrum and the mixing of several bands is possible in this region. C–N stretching vibration is assigned in the region 1400–1200 $cm^{-1}$ for aromatic amines [20]. In the present work, the calculated value is 1220 $cm^{-1}$, C–N Scissoring at the value of 614 $cm^{-1}$ in B3LYP respectively.

The heterocyclic aromatic compound of PGZE shows the presence of C–H stretching vibrations in the region 3100–3000 $cm^{-1}$, which is the characteristic region for the prepared recognition of C–H stretching vibration[21]. They are not appreciably affected by the nature of the substituent. In the present study, the calculated wavenumbers of C–H stretching modes are observed at 3189,3180,3168,3145 $cm^{-1}$ in HF and 3052,3047,3043,3020 $cm^{-1}$ B3LYP methods respectively. The experimental bands are observed at 2945 $cm^{-1}$in FT-Raman. The C–H in plane bending and C–H

out-of-plane bending vibrations are normally found in the range 1000–1300 $cm^{-1}$ and 750–1000 $cm^{-1}$ respectively in the aromatic compounds [22, 23]. In agreement with above literature data, the bands are observed at 1656,1472 $cm^{-1}$ in FT-IR spectrum and in FT-Raman at 1500,`481,1410,1150,1072 $cm^{-1}$ in the present study are due to C–H in - plane bending vibrations (Table 2). The C–H out-of-plane bending vibration observed at 952,1044$cm^{-1}$in IR bands and Raman bands observed at 974 $cm^{-1}$ are assigned. There is good agreement between theoretically computed C-H vibrational frequencies by B3LYP/6-311++G (d,p) method and experimental wave numbers.

According to Varsanyi, the bands are of variable intensity and are observed in the regions 1625–1590 1590–1575, 1540–1470, 1465–1430 and 1380–1280 $cm^{-1}$. The benzene and its derivatives of the vibrational spectra, the ring stretching vibrations are very prominent[24]. The actual positions of these modes are not influenced significantly by the nature of the substituents but by the relative positions of substitution around the ring system[25].In our present study, the wavenumber computed at 1634, 1644 and 1652 $cm^{-1}$by B3LYP/6-311++G(d,p) method (mode Nos. 104,105 and 106) are assigned to C-C and C-H stretching vibration for PGZE molecule and they show good agreement with recorded at 1656 $cm^{-1}$ in FT-IR spectrum. It may be pointed out that in-plane deformation vibrations are at higher wavenumbers than the out-of-plane vibrations.

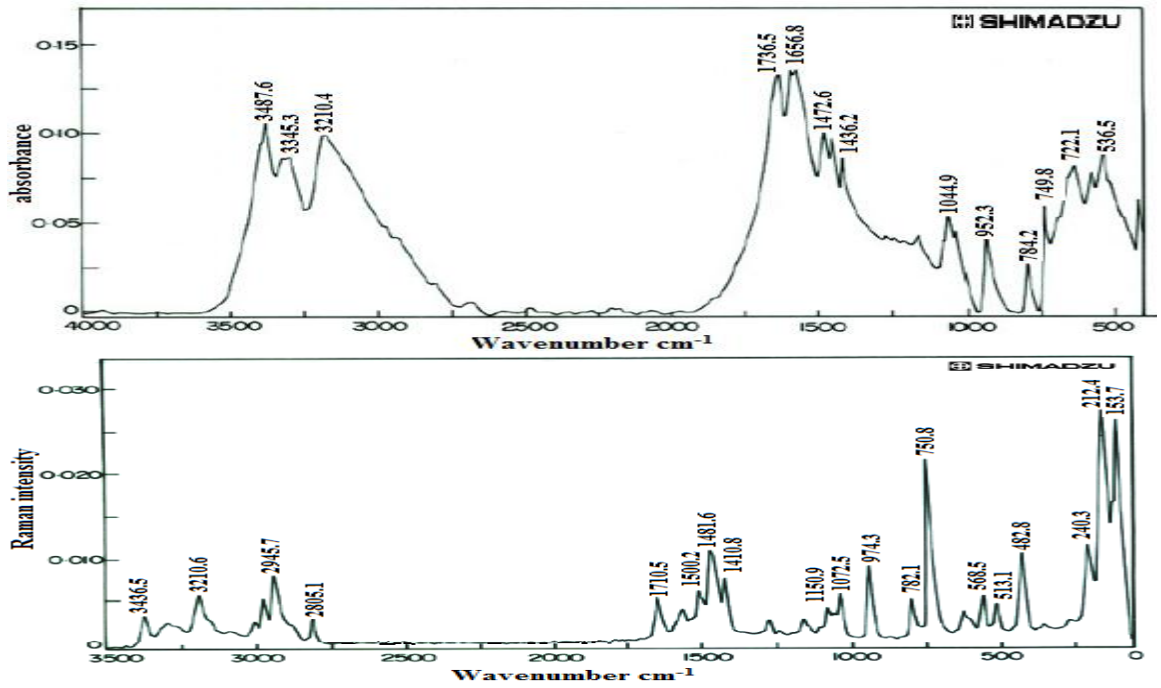


**Fig.2.FT-IR and FT-Raman spectrum of PGZE**

**Table 2: Experimental (FT-IR, FT-Raman) and theoretical Frequencies (infrared intensities ($I^{IR}$), Raman scattering activities ($S^{Ra}$) and Raman intensities ($I^{RA}$) of PGZE molecule computed by HF/6-311++G (d,p) and B3LYP/6-311++G(d,p) methods.**

| S.No. | Experimental Frequencies | | HF/6-311++ (d,p) | | | | B3LYP/6-311++(d,p) | | | | Vibrational assignments |
|---|---|---|---|---|---|---|---|---|---|---|---|
| | FT-IR | FT-Raman | scaled | $I^{IR}$ | $S^{Ra}$ | $I^{RA}$ | scaled | $I^{IR}$ | $S^{Ra}$ | $I^{RA}$ | |
| 1. | | | 8 | 1.11 | 4.44 | 4315.6 | 21 | 0.23 | 1.62 | 596.55 | Thiazolidinedione ring out-of plane bending |
| 2. | | | 11 | 0.68 | 1.07 | 755.42 | 40 | 0.40 | 0.14 | 26.85 | $CH_3$ Rocking |
| 3. | | | 24 | 0.39 | 1.19 | 382.94 | 63 | 1.36 | 1.15 | 138.65 | Ring deformation |
| 4. | | | 30 | 0.16 | 3.95 | 1014.2 | 84 | 1.00 | 2.2 | 197.14 | Ring torsion (phenyl) |
| 5. | | | 40 | 0.46 | 1.06 | 203.27 | 92 | 0.39 | 1.27 | 103.55 | Ring deformation |
| 6. | | | 44 | 0.27 | 2.12 | 368.95 | 101 | 1.63 | 3.79 | 280.40 | Ring twisting |
| 7. | | | 46 | 0.18 | 2.07 | 344.29 | 127 | 0.13 | 1.76 | 102.40 | $CH_3$ Rocking |
| 8. | | | 65 | 1.45 | 1.1 | 128.43 | 136 | 1.18 | 0.62 | 33.56 | Ring torsion (phenyl) |
| 9. | | 153.7 | 74 | 0.40 | 1.3 | 132.80 | 154 | 0.06 | 2.43 | 115.24 | Ring torsion (phenyl) |
| 10. | | | 108 | 0.14 | 0.49 | 33.80 | 174 | 5.10 | 1.4 | 58.26 | $CH_2$ Rocking |
| 11. | | | 118 | 4.39 | 0.56 | 35.20 | 186 | 0.61 | 0.98 | 37.95 | Ring deformation |
| 12. | | | 163 | 1.74 | 1.16 | 51.77 | 199 | 11.1 | 0.78 | 28.07 | C-N out-of plane bending |
| 13. | | | 165 | 5.49 | 1.95 | 85.90 | 205 | 4.85 | 0.68 | 23.70 | $CH_2$ Rocking |
| 14. | | 212.4 | 178 | 8.20 | 0.69 | 28.02 | 217 | 1.04 | 0.72 | 23.58 | Ring deformation |
| 15. | | | 186 | 1.64 | 1.86 | 72.03 | 228 | 0.72 | 1.95 | 60.49 | $CH_3$ Rocking |
| 16. | | 240.3 | 228 | 0.53 | 0.07 | 2.17 | 249 | 0.94 | 1.07 | 30.11 | $CH_3$ twisting |
| 17. | | | 242 | 4.90 | 0.9 | 26.14 | 271 | 1.33 | 1.72 | 44.05 | Ring deformation |
| 18. | | | 284 | 0.19 | 0.98 | 23.81 | 277 | 0.81 | 1.43 | 35.74 | Ring breathing (phenyl) |
| 19. | | | 305 | 0.58 | 1.22 | 27.35 | 304 | 0.37 | 0.2 | 4.50 | Ring deformation |
| 20. | | | 341 | 2.75 | 0.78 | 15.39 | 330 | 0.23 | 2.06 | 42.22 | Ring deformation |
| 21. | | | 380 | 2.89 | 0.91 | 15.84 | 345 | 9.21 | 0.7 | 13.63 | Ring deformation |
| 22. | | | 400 | 29.15 | 3.56 | 58.35 | 368 | 17.0 | 1.98 | 35.78 | C-O out-of plane bending |
| 23. | | | 424 | 4.34 | 2.3 | 35.19 | 405 | 2.43 | 0.04 | 0.65 | $CH_2$ out-of plane bending |
| 24. | | | 431 | 0.56 | 2.42 | 36.31 | 409 | 1.74 | 3.34 | 53.33 | $CH_2$ out-of plane bending |
| 25. | | | 449 | 1.69 | 0.25 | 3.57 | 420 | 7.42 | 0.52 | 8.05 | Pyridine out-of plane bending |
| 26. | | | 476 | 0.02 | 0.01 | 0.13 | 437 | 0.33 | 1.69 | 24.94 | Phenyl out-of plane bending |
| 27. | | | 479 | 7.38 | 0.83 | 10.97 | 440 | 0.98 | 0.26 | 3.81 | Phenyl out of plane bending |
| 28. | | 482.8 | 492 | 3.55 | 8.28 | 105.90 | 480 | 2.38 | 3.14 | 41.39 | Pyridine out of plane bending |
| 29. | | | 510 | 1.50 | 1.82 | 22.27 | 486 | 2.39 | 3.74 | 48.55 | Ring deformation (Pyridine) |
| 30. | | | 548 | 22.2 | 2.84 | 31.80 | 493 | 1.35 | 5.47 | 69.79 | S-O Scissoring |
| 31. | | 513.1 | 552 | 1.93 | 3.79 | 42.05 | 510 | 12.5 | 1.79 | 21.91 | Thiazolidinedione deformation |
| 32. | 536 | 568.5 | 586 | 30.0 | 2.02 | 20.79 | 566 | 14.2 | 0.34 | 3.66 | Ring Wagging (Phenyl) |
| 33. | | | 632 | 2.74 | 20.3 | 189.71 | 583 | 25.3 | 0.49 | 5.08 | Ring Wagging (Phenyl) |
| 34. | | | 639 | 18.6 | 5.87 | 54.08 | 614 | 7.14 | 19.7 | 191.0 | C-N Scissoring |

| | | | | | | | | | | | |
|---|---|---|---|---|---|---|---|---|---|---|---|
| | | | | | | | | | | 6 | |
| 35. | | | 660 | 1.29 | 1.16 | 10.25 | 625 | 7.27 | 0.53 | 5.02 | C-O out-of plane bending |
| 36. | | | 667 | 13.2 | 0.5 | 4.36 | 631 | 14.2 | 0.32 | 3.00 | Ring Wagging (Phenyl) |
| 37. | | | 698 | 25.2 | 10.2 | 83.74 | 674 | 6.29 | 5.93 | 50.97 | Ring deformation (Pyridine) |
| 38. | | | 716 | 1.03 | 6.91 | 54.85 | 684 | 7.34 | 7.6 | 64.08 | Ring deformation (Pyridine) |
| 39. | | | 721 | 5.26 | 7.18 | 56.46 | 685 | 6.10 | 7.04 | 59.25 | Ring deformation (Phenyl) |
| 40. | 722 | | 744 | 30.3 | 3.19 | 24.05 | 728 | 0.18 | 0.43 | 3.34 | Ring deformation (Phenyl) |
| 41. | 748 | 750.8 | 773 | 33.8 | 3.91 | 28.00 | 745 | 42.3 | 12.3 | 92.58 | S-C stretching |
| 42. | | | 789 | 23.7 | 3.35 | 23.33 | 766 | 14.2 | 0.46 | 3.33 | Pyridine out of plane bending |
| 43. | 784 | 782.1 | 812 | 34.2 | 2.94 | 19.68 | 786 | 20.0 | 3.49 | 24.43 | Pyridine in plane bending |
| 44. | | | 825 | 93.4 | 3.13 | 20.50 | 791 | 22.6 | 3.51 | 24.36 | Pyridine in plane bending |
| 45. | | | 849 | 14.7 | 2.33 | 14.66 | 808 | 6.12 | 0.07 | 0.47 | $CH_3$ out-of plane bending |
| 46. | | | 865 | 3.27 | 1.13 | 6.93 | 816 | 68.8 | 7.94 | 52.79 | N-H in plane bending |
| 47. | | | 871 | 11.5 | 8.05 | 48.87 | 825 | 3.13 | 0.89 | 5.83 | Pyridine out of plane bending |
| 48. | | | 904 | 4.45 | 3.16 | 18.20 | 849 | 3.49 | 27 | 145.02 | C-H out-plane bending |
| 49. | | | 908 | 7.22 | 5.57 | 31.88 | 862 | 2.40 | 20.8 | 128.14 | C-H out-plane bending |
| 50. | | | 937 | 6.70 | 54.9 | 300.35 | 869 | 13.5 | 1.69 | 10.29 | C-H out-plane bending (Phenyl) |
| 51. | | | 950 | 14.7 | 0.8 | 4.29 | 880 | 52.7 | 1.34 | 8.02 | C-H out-plane bending |
| 52. | | | 956 | 66.0 | 0.62 | 3.29 | 882 | 45.0 | 0.91 | 5.43 | C-H out-plane bending (Pyridine) |
| 53. | | | 970 | 25.5 | 3.08 | 16.02 | 927 | 2.81 | 5.53 | 30.72 | C-H out-plane bending |
| 54. | 952.3 | | 1029 | 7.53 | 4.39 | 20.93 | 950 | 2.53 | 7.09 | 38.02 | C-H out-plane bending, C-C stretching |
| 55. | | 974.3 | 1043 | 4.13 | 13.5 | 63.09 | 988 | 1.81 | 1.09 | 5.52 | C-H out-plane bending |
| 56. | | | 1049 | 8.52 | 4.28 | 19.83 | 994 | 5.00 | 1.97 | 9.89 | C-H out-plane bending |
| 57. | | | 1068 | 1.34 | 1.46 | 6.58 | 1003 | 2.55 | 5.19 | 25.71 | C-H out-plane bending, C-C stretching |
| 58. | | | 1089 | 0.64 | 0.25 | 1.09 | 1014 | 1.93 | 1.01 | 4.92 | C-H out-plane bending (Phenyl) |
| 59. | | | 1116 | 0.13 | 0.16 | 0.67 | 1016 | 1.34 | 8.07 | 39.22 | C-H out-plane bending |
| 60. | | | 1118 | 53.0 | 1.83 | 7.70 | 1027 | 1.29 | 0.07 | 0.33 | C-H out-plane bending (Phenyl) |
| 61. | | | 1122 | 0.21 | 0.12 | 0.50 | 1029 | 0.18 | 0.68 | 3.24 | C-H out-plane bending (Pyridine) |
| 62. | 1044 | | 1124 | 40.7 | 4.98 | 20.77 | 1056 | 2.65 | 0.18 | 0.83 | C-H out-plane bending (Phenyl) |
| 63. | | | 1130 | 27.5 | 2.7 | 11.17 | 1059 | 4.53 | 0.35 | 1.60 | C-H in-plane bending |
| 64. | | 1072.5 | 1136 | 10.1 | 9.72 | 39.88 | 1080 | 15.0 | 2.29 | 10.15 | C-H in-plane bending |
| 65. | | | 1154 | 23.0 | 4.83 | 19.34 | 1085 | 7.42 | 13.3 | 58.55 | C-C stretching |
| 66. | | | 1177 | 5.72 | 9.51 | 36.92 | 1115 | 6.84 | 4.98 | 21.03 | C-H in-plane bending |
| 67. | | | 1195 | 7.21 | 4.04 | 15.31 | 1117 | 8.50 | 9.5 | 40.00 | C-H in-plane bending |
| 68. | | | 1202 | 5.84 | 7.28 | 27.34 | 1136 | 43.2 | 15.6 | 64.00 | C-H in-plane bending |
| 69. | | 1150.9 | 1224 | 13.1 | 0.49 | 1.79 | 1163 | 4.79 | 2.5 | 9.89 | C-H in-plane bending (Phenyl) |
| 70. | | | 1232 | 7.04 | 1.14 | 4.12 | 1189 | 4.87 | 3.61 | 13.79 | C-H in-plane bending |
| 71. | | | 1259 | 17.5 | 5.68 | 19.80 | 1213 | 55.1 | 2.17 | 8.03 | C-H in-plane bending |
| 72. | | | 1299 | 154. | 1.99 | 6.59 | 1220 | 76.1 | 4.09 | 15.00 | C-N stretching |

| | | | | | | | | | | | |
|---|---|---|---|---|---|---|---|---|---|---|---|
| | | | | 7 | | | | | | | |
| 73. | | | 1300 | 7.47 | 3.5 | 11.58 | 1241 | 20.3 | 13.6 | 48.53 | C-H stretching |
| 74. | | | 1311 | 24.7 | 4.68 | 15.27 | 1248 | 12.6 | 3.98 | 14.07 | C-H in-plane bending |
| 75. | | | 1327 | 87.0 | 16.1 | 51.50 | 1263 | 1.02 | 36.4 | 126.25 | C-H in-plane bending, C-C stretching |
| 76. | | | 1330 | 2.49 | 27 | 86.04 | 1268 | 9.86 | 28.3 | 97.53 | C-H in-plane bending, C-C stretching |
| 77. | | | 1341 | 6.10 | 4.16 | 13.08 | 1280 | 11.9 | 1.85 | 3.39 | C-H in-plane bending, C-C stretching |
| 78. | | | 1348 | 20.0 | 9.79 | 30.51 | 1299 | 174.4 | 2.46 | 8.15 | C-H in-plane bending |
| 79. | | | 1372 | 50.6 | 0.39 | 1.18 | 1302 | 7.20 | 6.79 | 22.41 | C-H in-plane bending |
| 80. | | | 1389 | 322.4 | 12.9 | 38.22 | 1306 | 3.83 | 3.5 | 11.49 | C-H in-plane bending |
| 81. | | | 1400 | 115.4 | 6.1 | 17.83 | 1322 | 3.17 | 5.98 | 19.25 | $CH_2$ wagging |
| 82. | | | 1409 | 0.64 | 8.7 | 25.16 | 1328 | 229.7 | 4.74 | 15.14 | C-H in-plane bending |
| 83. | | | 1429 | 9.24 | 8.34 | 23.54 | 1331 | 34.3 | 3.39 | 10.79 | $CH_3$ in-plane bending |
| 84. | | | 1439 | 20.5 | 6.58 | 18.35 | 1344 | 251.5 | 37.5 | 117.43 | C-H in-plane bending, C-O stretching |
| 85. | | | 1443 | 238.7 | 2.27 | 6.30 | 1359 | 2.31 | 2.25 | 6.92 | C-H in-plane bending |
| 86. | | | 1449 | 3.79 | 12.2 | 33.62 | 1373 | 4.89 | 4.56 | 13.78 | C-H in-plane bending |
| 87. | | | 1481 | 6.61 | 0.54 | 1.43 | 1390 | 0.84 | 17.2 | 50.90 | C-H in-plane bending, $CH_2$ wagging |
| 88. | | | 1488 | 2.97 | 1.89 | 4.97 | 1396 | 3.61 | 2.61 | 7.67 | C-H in-plane bending, $CH_2$ twisting |
| 89. | | | 1501 | 5.40 | 10.6 | 27.47 | 1406 | 0.24 | 30.4 | 88.23 | $CH_2$ wagging |
| 90. | | 1410.8 | 1520 | 16.2 | 21.3 | 53.99 | 1408 | 1.26 | 19.5 | 56.46 | C-H in-plane bending |
| 91. | | | 1548 | 15.8 | 0.55 | 1.35 | 1423 | 4.57 | 9.42 | 26.78 | N-H in-plane bending |
| 92. | 1436 | | 1558 | 2.14 | 5.04 | 12.22 | 1444 | 11.5 | 3.44 | 9.54 | $CH_3$ stretching |
| 93. | | | 1565 | 3.14 | 2.16 | 5.20 | 1457 | 14.2 | 2.98 | 8.14 | C-H in-plane bending, $CH_2$ wagging |
| 94. | | | 1571 | 32.2 | 6.56 | 15.68 | 1460 | 5.81 | 0.99 | 2.69 | $CH_3$ wagging |
| 95. | 1472 | 1481.6 | 1577 | 9.01 | 8.81 | 20.91 | 1462 | 0.55 | 0.32 | 0.87 | C-H in-plane bending |
| 96. | | 1500.2 | 1634 | 12.9 | 15.5 | 34.48 | 1530 | 25.5 | 10.2 | 25.56 | C-H in-plane bending |
| 97. | | | 1644 | 12.0 | 22.9 | 50.37 | 1532 | 13.4 | 6.75 | 16.87 | C-H in-plane bending |
| 98. | | | 1646 | 4.32 | 13.8 | 30.28 | 1544 | 59.8 | 16.9 | 41.66 | $CH_3$Scirroring |
| 99. | | | 1647 | 9.50 | 19.5 | 42.74 | 1547 | 12.2 | 17.2 | 42.25 | C-H in-plane bending |
| 100. | | | 1660 | 56.2 | 8.98 | 19.40 | 1550 | 14.1 | 12.2 | 29.87 | $CH_3$Scirroring |
| 101. | | | 1662 | 10.5 | 1.67 | 3.60 | 1556 | 22.6 | 10.4 | 25.28 | C-H in-plane bending |
| 102. | | | 1680 | 176.2 | 5.61 | 11.85 | 1560 | 15.8 | 0.56 | 1.36 | C-H in-plane bending |
| 103. | | | 1692 | 16.8 | 8.94 | 18.64 | 1582 | 135.3 | 3.9 | 9.20 | C-H in-plane bending |
| 104. | | | 1743 | 16.0 | 5.21 | 10.27 | 1634 | 2.27 | 33.9 | 75.41 | C-H in-plane bending, C=C stretching |
| 105. | | | 1757 | 15.3 | 9.41 | 18.26 | 1644 | 11.5 | 15.3 | 33.65 | C=C stretching |
| 106. | | | 1790 | 39.8 | 58.3 | 109.15 | 1652 | 22.2 | 25.3 | 54.49 | C-H in-plane bending (Pyridine) |
| 107. | 1656 | | 1800 | 77.8 | 84.6 | 156.68 | 1655 | 67.9 | 80.4 | 174.67 | C-H in-plane bending (Phenyl) |
| 108. | 1736 | 1710.5 | 1866 | 949.3 | 1.92 | 3.31 | 1742 | 829.8 | 5.97 | 11.78 | C=O stretching |
| 109. | | | 1895 | 263.7 | 26.3 | 43.99 | 1779 | 216.4 | 57.5 | 108.94 | C=O stretching |
| 110. | | 2945.7 | 3145 | 46.3 | 87.3 | 42.45 | 3020 | 26.0 | 96.2 | 52.73 | C-H stretching |
| 111. | | | 3168 | 36.9 | 166.7 | 79.29 | 3043 | 11.2 | 101.7 | 54.53 | $CH_2$ stretching |

| | | | | | | | | | | | |
|---|---|---|---|---|---|---|---|---|---|---|---|
| 112. | | | 3180 | 11.9 | 112.8 | 53.04 | 3047 | 30.3 | 182.3 | 97.37 | C-H stretching |
| 113. | | | 3189 | 35.6 | 66.8 | 31.14 | 3052 | 31.0 | 107.6 | 57.20 | $CH_3$ stretching |
| 114. | | | 3190 | 17.2 | 90.3 | 42.06 | 3054 | 5.36 | 97.5 | 51.73 | C-H asymmetric stretching |
| 115. | | | 3194 | 4.59 | 105.7 | 49.04 | 3065 | 3.79 | 45.1 | 23.68 | C-H asymmetric stretching |
| 116. | | | 3223 | 80.6 | 139.1 | 62.77 | 3071 | 6.15 | 100.4 | 52.41 | C-H asymmetric stretching |
| 117. | | | 3229 | 8.03 | 63.3 | 28.40 | 3073 | 67.9 | 188.7 | 98.31 | C-H asymmetric stretching |
| 118. | | | 3230 | 59.5 | 12.5 | 5.60 | 3092 | 1.90 | 29.5 | 15.09 | C-H asymmetric stretching |
| 119. | | | 3232 | 6.26 | 53.6 | 23.98 | 3097 | 12.6 | 63.4 | 32.28 | C-H asymmetric stretching |
| 120. | | | 3265 | 31.1 | 8.81 | 3.82 | 3117 | 54.9 | 159.7 | 79.77 | C-H asymmetric stretching |
| 121. | | | 3273 | 3.90 | 34.8 | 14.97 | 3118 | 30.1 | 12.6 | 6.29 | C-H symmetric stretching |
| 122. | | | 3323 | 21.1 | 70.5 | 28.91 | 3176 | 13.7 | 76.3 | 36.02 | C-H symmetric stretching |
| 123. | | | 3328 | 20.1 | 73.7 | 30.07 | 3178 | 8.30 | 39.2 | 18.47 | C-H symmetric stretching |
| 124. | | | 3340 | 18.9 | 42.4 | 16.94 | 3182 | 18.2 | 43.4 | 20.37 | C-H symmetric stretching |
| 125. | | | 3341 | 35.1 | 72.8 | 29.34 | 3183 | 19.6 | 83.5 | 39.15 | C-H symmetric stretching |
| 126. | | | 3361 | 14.3 | 126.9 | 50.17 | 3195 | 6.64 | 54.3 | 25.17 | C-H symmetric stretching |
| 127. | | | 3377 | 9.84 | 96.7 | 37.65 | 3200 | 2.63 | 156.1 | 72.01 | C-H symmetric stretching |
| 128. | 3210 | 3210.6 | 3381 | 11.1 | 110.3 | 42.78 | 3207 | 9.29 | 128.1 | 58.70 | C-H symmetric stretching |
| 129. | 3487 | 3436.5 | 3851 | 105.3 | 144.5 | 35.54 | 3576 | 83.5 | 214.7 | 69.00 | N-H symmetric stretching |

### *3.3 NBO analysis*

Natural Bond Orbital (NBO) analysis provides the most important interactions between 'filled' (donors or Lewis−type) and 'empty' (acceptors or non−Lewis) are reported. The second-order Fock matrix was carried out to evaluate the donor–acceptor interactions in the NBO analysis[26.] Delocalization of electrons present in occupied Lewis type (bonding or non-bonding) orbitals and unoccupied non-Lewis type (anti-bonding) orbitals shows significant donor-acceptor interaction. DFT method predicts satisfactorily the extent of delocalization [27] in organic molecules and the various interactions in molecule from filled orbitals of one atom to vacant orbital of another is investigated by NBO analysis. Larger the E(2) value, the more intensive is the interaction between electron donors and electron acceptors and greater is the tendency of electron donation from donor to acceptor. Consequently, larger is the extent of conjugation in the entire molecular system. The 30 interactions of the two lone-pairs LP(1) and LP(2) of the molecule. In sulpher, 6 interactions of the two lone-pairs LP(2) and LP(1) of oxygen and nitrogen are assessed using NBO analysis and the results are presented as supplementary data in Table 3. It is found that of the nitrogen atoms only N3 lone pairs are involved in the interaction with neighboring atoms. They are n1 N3→$\sigma^*$ C2-N3 (232.3kJ/mol). There are 30 interactions involving these 6 nitrogen atoms as donors. They interact mainly with orbitals of C18-C19, C25-C26 and C21-C22in the benzene ring.

**Table 3: Second order perturbation theory analysis of Fock matrix in NBO basis of PGZE.**

| Donor (i) | Type | ED (e) | Acceptor (j) | Type | E (2) [a] kJ mol$^{-1}$ | E (j) – E (i)[b] kJ mol$^{-1}$ | F (i,j)[c] kJ mol$^{-1}$ |
|---|---|---|---|---|---|---|---|
| $S_1$ | $n_1$ | 1.35 | $C_2$-$N_3$ | $\sigma^*$ | 216.8 | 21.4 | 12.6 |
| $S_1$ | $n_1$ | 1.35 | $C_4$-$C_5$ | $\sigma^*$ | 209.2 | 10.1 | 9.4 |
| $S_1$ | $n_2$ | 1.35 | $C_2$-$O_6$ | $\sigma^*$ | 8.09 | 26.8 | 3.6 |
| $S_1$ | $n_2$ | 1.35 | $C_5$-$C_8$ | $\sigma^*$ | 8.19 | 25.5 | 3.7 |
| $S_1$ | $n_2$ | 1.35 | $C_5$-$H_{27}$ | $\sigma^*$ | 53.5 | 16.3 | 4.9 |
| $S_1$ | $n_2$ | 1.35 | $C_8$-$H_{29}$ | $\sigma^*$ | 3.76 | 78.7 | 3.1 |
| $N_3$ | $n_1$ | 1.98 | $C_2$-$O_6$ | $\sigma^*$ | 8.01 | 101.3 | 4.1 |
| $N_3$ | $n_1$ | 1.98 | $C_4$-$O_7$ | $\sigma^*$ | 83.7 | 32.2 | 7.5 |
| $O_6$ | $n_1$ | 1.85 | $S_1$-$C_2$ | $\sigma^*$ | 16.8 | 40.5 | 3.7 |
| $O_6$ | $n_1$ | 1.85 | $C_2$-$N_3$ | $\sigma^*$ | 45.6 | 3.2 | 5.7 |
| $O_6$ | $n_2$ | 1.81 | $S_1$-$C_2$ | $\sigma^*$ | 15.5 | 36.7 | 1.9 |
| $O_6$ | $n_2$ | 1.81 | $C_2$-$N_3$ | $\sigma^*$ | 120.8 | 46.3 | 9.4 |
| $O_7$ | $n_1$ | 1.81 | $N_7$-$C_4$ | $\sigma^*$ | 81.9 | 31.9 | 7.1 |
| $O_7$ | $n_1$ | 1.98 | $C_4$-$C_5$ | $\sigma^*$ | 3.74 | 91.7 | 2.6 |
| $O_7$ | $n_2$ | 1.98 | $S_1$-$C_5$ | $\sigma^*$ | 8.5 | 101.3 | 4.1 |
| $O_7$ | $n_2$ | 1.85 | $C_2$-$N_3$ | $\sigma^*$ | 22.5 | 36.7 | 7.5 |
| $O_7$ | $n_2$ | 1.85 | $N_3$-$C_4$ | $\sigma^*$ | 18.2 | 46.3 | 3.8 |
| $O_7$ | $n_2$ | 1.85 | $C_4$-$C_5$ | $\sigma^*$ | 32.7 | 32.8 | 5.7 |
| $O_{15}$ | $n_1$ | 1.84 | $C_{11}$-$C_{12}$ | $\sigma^*$ | 6.78 | 36.7 | 1.9 |
| $O_{15}$ | $n_1$ | 1.84 | $C_{16}$-$C_{17}$ | $\sigma^*$ | 102.6 | 46.3 | 9.4 |
| $O_{15}$ | $n_1$ | 1.84 | $C_{16}$-$H_{34}$ | $\sigma^*$ | 41.3 | 31.9 | 7.1 |
| $O_{15}$ | $n_1$ | 1.93 | $C_{16}$-$H_{35}$ | $\sigma^*$ | 16.1 | 41.5 | 3.6 |
| $O_{15}$ | $n_1$ | 1.93 | $C_{17}$-$C_{18}$ | $\sigma^*$ | 10.5 | 51.2 | 2.9 |
| $O_{15}$ | $n_2$ | 1.93 | $C_{11}$-$C_{12}$ | $\sigma^*$ | 7.8 | 51.2 | 3 |
| $O_{15}$ | $n_2$ | 1.93 | $C_{16}$-$H_{34}$ | $\sigma^*$ | 2.0 | 37.6 | 1.3 |
| $O_{15}$ | $n_2$ | 1.93 | $C_{16}$-$H_{35}$ | $\sigma^*$ | 31.5 | 78.2 | 6.3 |
| $N_{23}$ | $n_1$ | 1.93 | $C_{17}$-$C_{18}$ | $\sigma^*$ | 22.6 | 87.8 | 2.7 |
| $N_{23}$ | $n_1$ | 1.93 | $C_{18}$-$C_{19}$ | $\sigma^*$ | 5.3 | 71.4 | 2.1 |
| $N_{23}$ | $n_1$ | 1.95 | $C_{21}$-$C_{22}$ | $\sigma^*$ | 3.0 | 90.7 | 5.6 |
| $N_{23}$ | $n_1$ | 1.95 | $C_{22}$-$H_{40}$ | $\sigma^*$ | 21.3 | 73.3 | 4.4 |

[a] E(2) = Interaction energy.

[b] E (j) – E (i) = Energy difference between donor 'i' and acceptor 'j' NBO.

[c] F(i,j) is the Fock matrix element between i and j NBO.

## *3.4 NLO properties and dipole moment*

This Non-linear optical (NLO) study includes electronic dipole moment, molecular polarizability, the anisotropy of polarizability and molecular first hyperpolarizability molecule. To obtain polarizability and hyperpolarizability tensors ($\alpha_{xx}$, $\alpha_{yy}$, $\alpha_{zz}$ $\alpha_{xz}$ and $\beta_{xxx}$, $\beta_{xxy}$, $\beta_{xyy}$, $\beta_{yyy}$, $\beta_{xxz}$, $\beta_{yyz}$, $\beta_{xzz}$, $\beta_{yzz}$, $\beta_{zzz}$), a frequency job output file of Gaussian [9] is employed. The units α and β values of Gaussian output are in atomic units (a.u.) and they are converted into electronic units (esu) using the conversion factors;α; 1 a.u. = 0.1482 x $10^{-24}$ esu andβ; 1 a.u. = 8.6393 x $10^{-33}$ esu. The mean polarizability (α), the anisotropy of polarizability ( $\Delta\alpha$ ) and the average value of the first hyperpolarizability ($\beta$) can be calculated using the equations (2-4).

Mean polarisability $\alpha_o = \frac{\alpha_{xx} + \alpha_{yy} + \alpha_{zz}}{3}$ …….. (2)

Anisotropic polarisability $(\Delta\alpha) = 2^{-1/2}\left[(\alpha_{xx} - \alpha_{yy})^2 + (\alpha_{yy} - \alpha_{zz})^2 + (\alpha_{zz} - \alpha_{xx})^2 + 6\alpha_{xz}^2\right]^{1/2}$ …. (3)

First-order polarisability $\beta_{tot} = \left(\beta_x^2 + \beta_y^2 + \beta_z^2\right)^{1/2}$ …… (4)

Where,

$$\beta_x = \beta_{xxx} + \beta_{yyy} + \beta_{zzz}$$
$$\beta_y = \beta_{yyy} + \beta_{xxy} + \beta_{yzz}$$
$$\beta_z = \beta_{zzz} + \beta_{xxz} + \beta_{yyz}$$

The parameters described above and electronic dipole moment {($\mu_i$) *i* = x, y, z)} and total dipole moment $\mu_{tot}$ for the molecule are gathered and listed in Table 4. The total dipole moment can be calculated using equation (5).

$\mu_{tot} = \left(\mu_x^2 + \mu_y^2 + \mu_z^2\right)^{1/2}$ …… (5)

Generally, molecules with large values of dipole moment, molecular polarizability, and hyperpolarizability exhibit NLO properties. The calculated net dipole moment of is 4.93D in HF method and 4.87 D in B3LYP/6-311++G(d,p) method. The high component dipole moment is observed for $\mu_z$ in HF/6-311++G(d,p) method. The value of $\mu_x$ is the smallest one at –4.88 D and ─4.83 D. The calculated polarizability and anisotropy of the polarizability of the title molecule are almost the same values in the HF and DFT methods. The magnitude of the first hyperpolarizability $\beta_{tot}$, is one of the very important factors in an NLO system. The highest value of the first hyperpolarizability ( $\beta_{tot}$ ) (435.02x$10^{-33}$ esu) is obtained by the method of DFT/6-311++G(d,p) method. It is interesting to note that the first hyperpolarizability of PGZE is more than fifty times greater than that of urea, one of the prototypical molecules used in the study of the NLO properties. On the basis of high values of dipole moment and first hyperpolarizability it may be concluded that can possess NLO properties.

**Table 4: Component dipole moment, net dipole moment $\mu_{tot}$ (D), component polarizability, mean polarizability $\alpha_o$ /$10^{-22}$ esu, anisotropy polarizability $\Delta\alpha$ /$10^{-25}$ esu and component and total first hyperpolarizability $\beta_{tot}$ /$10^{-31}$ esu values for PGZE.**

| Parameters | HF/6-311++G(d,p) | B3LYP/6-311++G(d,p) |
|---|---|---|
| $\mu_x$ | -4.88 | -4.83 |
| $\mu_y$ | 0.33 | -0.19 |
| $\mu_z$ | 0.62 | -0.59 |
| $\mu_{tot}$ | 4.93 | 4.87 |
| $\alpha_{xx}$ | -139.88 | -132.37 |
| $\alpha_{yy}$ | -174.09 | -169.84 |
| $\alpha_{zz}$ | -154.62 | -154.33 |
| $\alpha_{xy}$ | 16.2 | -13.61 |
| $\alpha_{xz}$ | -7.14 | 7.53 |
| $\alpha_{yz}$ | 9.71 | 9.05 |
| $\alpha_o$ | -156.19 | -152.78 |
| $\Delta_\alpha$ | -63.24 | -70.23 |
| $\beta_{xxx}$ | -330.88 | -284.43 |
| $\beta_{xxy}$ | -45.34 | 46.59 |
| $\beta_{xxz}$ | 38.35 | -30.68 |
| $\beta_{yyy}$ | 56.86 | -48.22 |
| $\beta_{yyz}$ | -4.82 | 4.69 |
| $\beta_{xyy}$ | -97.48 | -87.02 |
| $\beta_{xyz}$ | 20.66 | 17.02 |
| $\beta_{xzz}$ | -4.88 | -3.82 |
| $\beta_{zzz}$ | 5.17 | -4.57 |
| $\beta_{yzz}$ | -4.52 | 3.79 |
| $\beta_{tot}$ | 435.02 | 376.51 |

## *3.5 Atomic Charge Distributions in PGZE*

The charge distributions calculated by the Mulliken method [28] for the equilibrium geometry are given in Table 5. The charge distribution in the molecule has an important influence on the vibrational frequencies[29]. The calculated results reveal that the negative charge is delocalized on specific carbon, one sulfur, three oxygen and two nitrogen atoms. The total charge of the investigated compound is zero as it is neutral. In the molecule, all hydrogen atoms and some carbon atoms possess positive charges. Most of the carbon atoms in the molecule have negative charges. Very similar values of positive charges are noticed for the hydrogen atoms of the CH3 group and oxygen atoms of a CH2 group. It may be noted that in the thiazole ring N3, O6 and O7 atoms and pyridine ring N23 also have negative charges while C2, C4, C18 and C22 carbon atoms are positive charges. This suggests that there is resonance involving a lone pair of electrons of nitrogen atoms. Most of the benzene ring carbon atoms are negatively charged indicating intra-molecular conjugative electron interactions. For the hydrogen atoms, the differences in calculated charge are relatively smaller. Very smaller value of positive charges is observed for hydrogen atoms and negative charge observed for nitrogen atoms connected with carbon atoms of in benzene ring. The high values of positive charge are noticed for H26 indicating that these hydrogen atoms are involved in hydrogen bonding. The

charge increase at the hydrogen atoms taking part in hydrogen bonding is also a clear manifestation of hydrogen bonding. Large values of charge on N3 (negative) and H26 (positive) are due to intramolecular charge transfer. It is observed that the charges computed by HF method are more negative than those obtained by the B3LYP method. From the electronic charge distribution obtained in the present study, we can infer that it is an electrophile in the reaction then the reaction sites may be N3 which are electron deficient. On the other hand, it acts as a nucleophile in the inhibition reaction, then the electron-rich aromatic carbon atoms may site of drug action.

**Table 5: Atomic Charges at different positions of PGZE.**

| Atom | HF/6-311++G(d,p) | | B3LYP/6-311++G(d,p) | |
|---|---|---|---|---|
| | Natural charge | Mulliken charge | Natural charge | Mulliken charge |
| S1 | 0.2 | 0.28 | 0.14 | 0.37 |
| C2 | 0.55 | 0.47 | 0.66 | -0.55 |
| N3 | -0.69 | -0.84 | -0.72 | -0.46 |
| C4 | 0.64 | 0.83 | -0.78 | -0.44 |
| C5 | -0.36 | -0.64 | -0.33 | -0.74 |
| O6 | -0.48 | -0.48 | -0.62 | -0.56 |
| O7 | -0.56 | -0.49 | -0.64 | -0.59 |
| C8 | -0.41 | -0.4 | -0.36 | -0.41 |
| C9 | -0.07 | 0.02 | -0.08 | 0.02 |
| C10 | -0.17 | -0.13 | -0.15 | 0.71 |
| C11 | -0.29 | -0.19 | -0.28 | -0.18 |
| C12 | 0.29 | 0.37 | 0.37 | -0.19 |
| C13 | -0.22 | -0.2 | -0.22 | -0.45 |
| C14 | -0.2 | -0.13 | -0.16 | 0.32 |
| O15 | -0.51 | -0.71 | -0.62 | -0.12 |
| C16 | -0.07 | 0.02 | 0.05 | -0.21 |
| C17 | -0.41 | -0.42 | -0.37 | -0.19 |
| C18 | 0.19 | 0.28 | 0.23 | 0.31 |
| C19 | -0.21 | -0.24 | -0.23 | 0.4 |
| C20 | -0.19 | -0.04 | -0.13 | -0.01 |
| C21 | -0.08 | -0.09 | -0.07 | -0.21 |
| C22 | 0.08 | 0.1 | 0.09 | -0.45 |
| N23 | -0.44 | -0.52 | -0.51 | -0.14 |
| C24 | -0.37 | -0.43 | -0.34 | 0.07 |
| C25 | -0.56 | -0.46 | -0.5 | -0.54 |
| H26 | 0.41 | 0.41 | 0.44 | 0.29 |
| H27 | 0.25 | 0.28 | 0.22 | 0.22 |
| H28 | 0.22 | 0.2 | 0.19 | 0.24 |
| H29 | 0.24 | 0.24 | 0.21 | 0.2 |
| H30 | 0.21 | 0.18 | 0.2 | 0.19 |
| H31 | 0.22 | 0.2 | 0.21 | 0.24 |
| H32 | 0.22 | 0.19 | 0.21 | 0.2 |
| H33 | 0.21 | 0.17 | 0.19 | 0.2 |
| H34 | 0.19 | 0.17 | 0.15 | 0.19 |
| H35 | 0.18 | 0.2 | 0.17 | 0.19 |
| H36 | 0.23 | 0.21 | 0.2 | 0.21 |
| H37 | 0.23 | 0.19 | 0.19 | 0.26 |
| H38 | 0.2 | 0.18 | 0.2 | 0.18 |
| H39 | 0.2 | 0.17 | 0.2 | 0.2 |
| H40 | 0.19 | 0.18 | 0.18 | 0.2 |
| H41 | 0.2 | 0.18 | 0.18 | 0.19 |
| H42 | 0.19 | 0.18 | 0.18 | 0.2 |
| H43 | 0.2 | 0.17 | 0.18 | 0.19 |

| | | | | |
|---|---|---|---|---|
| H44 | 0.2 | 0.17 | 0.17 | 0.19 |
| H45 | 0.19 | 0.17 | 0.18 | 0.19 |

### *3.6 HOMO and LUMO analysis*

The highest occupied molecular orbital (HOMO) energy characterizes the ability of electron giving; LUMO lowest unoccupied molecular orbital (LUMO) energy characterizes the ability of electron accepting. The gap between HOMO (donor) and LUMO (acceptor) characterizes the molecular chemical stability and measure of electron conductivity. The HOMO and LUMO energies calculated by the basis sets with diffuse function are higher than those of the other basis sets. In most cases, the Organic molecules containing strongest bands in the Raman spectrum are weak in the IR spectrum and vice versa even in absence of inversion symmetry[30]. The energy gap (**ΔE**) shows that chemical reactivity and the level of conductivity of the molecule. That is the smaller value of **ΔE**, the easer electron transfers from HOMO orbital to LUMO orbital. HOMO, LUMO, and **ΔE** are well correlated with the drug potency for drug precursor molecules. The frontier molecular orbitals (FMOs) play important role in the optical and electric properties as well as in UV–vis spectra [31] of organic molecules. The FMOs of DDT-4 (HOMO–LUMO) with HF/6311++G(d,p) method showed at Figure 3 and Table 6. The biggest HOMO energy value is –0.192 eV and LUMO energy value are –0.2813eV calculated at B3LYP /6-311++G(d,p). According to the calculation, the energy band gap (**ΔE**) of the molecule is about 0.089eV.

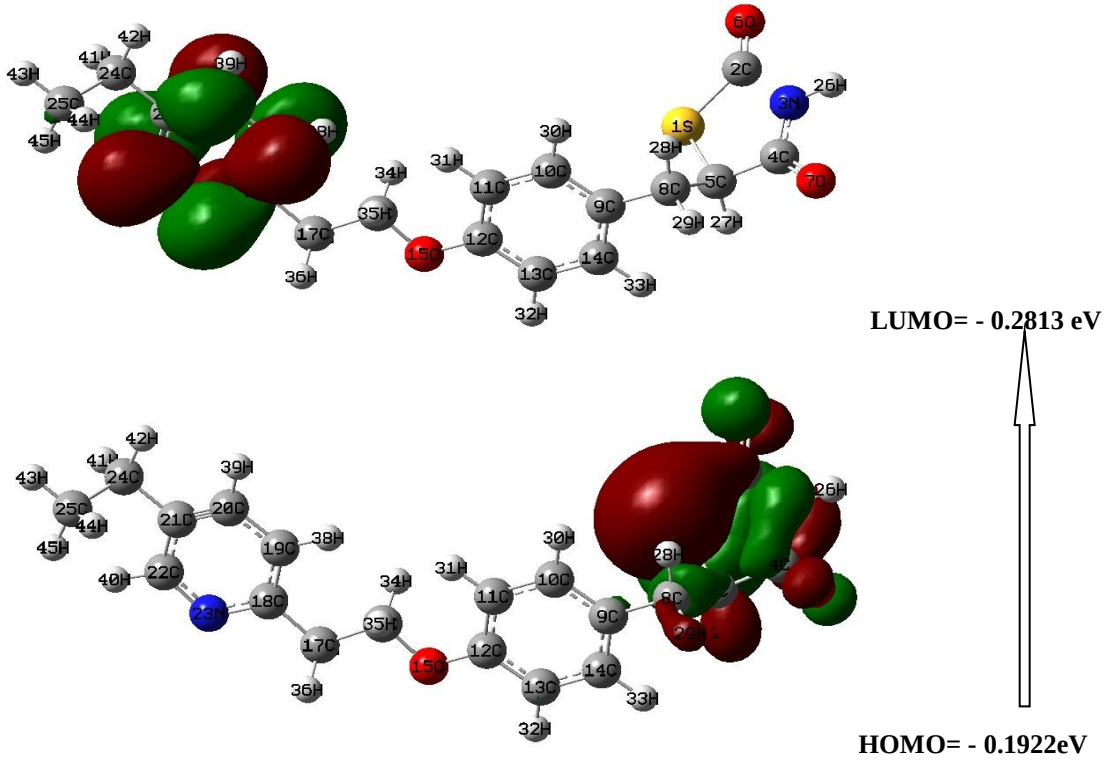


**Fig. 3: HOMO – LUMO energy diagram of PGZE; Energy gap ΔE = 0.0891eV**

**Table 6: HOMO, LUMO energy values, chemical hardness (η), electronegativity (χ), chemical potential (μ), electrophilicity index (ω) and softness (σ) of PGZE in gas phase.**

| Parameters | HF/6-311++G (d,p) | B3LYP/6-311++G(d,p) |
|---|---|---|
| $E_{total}$ (kJ/ $mol^{-1}$) | -7.6 x $10^5$ | -8.2 x$10^5$ |
| $E_{HOMO}$ (eV) | -0.25 | -0.28 |
| $E_{LUMO}$ (eV) | -0.12 | -0.19 |
| $\Delta E_{HOMO-LUMO}$ (eV) | 0.13 | 0.09 |
| Chemical hardness (η) | 4.7 | 3.2 |
| Electronegativity (χ) | 4.7 | 3.2 |
| Chemical potential (μ) (eV) | −3.6 | −2.8 |
| Electrophilicity index (ω) | 1.37 | 2.75 |
| Softness (σ) | 0.3 | 0.5 |

### *3.7 Global and local reactivity descriptors*

The electrical transport properties are related to the energy gap between HOMO and LUMO in inorganic and organic molecules. The global chemical reactivity descriptors of organic molecules such as hardness, chemical potential, softness, electronegativity, and electrophilicity index as well as local reactivity can be calculated from HOMO and LUMO energy values. Pauling introduced the concept of electronegativity as the power of an atom in a molecule to attract electrons towards it. Values of hardness (η), a chemical potential (μ), electronegativity (χ) and softness for are calculated using equations given by earlier workers [32,33,34,35,36]. Softness ($\sigma$) of a molecule that measures the extent of chemical reactivity. It is the reciprocal of hardness. Since is a closed-shell molecule,η, μ and χ are computed from ionization potential and electron affinity using Koopman's theorem (Table 6). The ionization energy and electron affinity were computed from HOMO and LUMO orbital energies. The ionization potential calculated by HF and B3LYP methods for DDT-4 is 15.467 eV and 8.734 eV respectively. Generally, a large HOMO–LUMO energy gap means a hard molecule and small HOMO– LUMO gap means a soft molecule. The stability of a molecule and its reactivity can be related to hardness. A molecule with least HOMO–LUMO energy gap (soft molecule) is more reactive. Parr et al. [32] have proposed electrophilicity index (ω) as a measure of energy lowering due to maximal electron flow between donor and acceptor. It is defined by equation [5].

$$\omega = \frac{\mu^2}{2\eta} \qquad \text{..... (5)}$$

Using the above equation electrophilicity index is calculated and it is shown in Table 6. The usefulness of this new reactivity parameter has been recently demonstrated in understanding the toxicity of various pollutants in terms of their reactivity and site selectivity[37,38,39,40,41]. Domingo *et al*. proposed that the electrophilic index indicates the electrophilic site in organic reactions[42]. A strong and more reactive nucleophile is characterized by a lower value of $\mu$. On the other hand, a good

electrophile is characterized by a high value of ω. The electronegativity and hardness are used extensively are to predict the reactivity and aromatic behavior in organic compounds [43]. In the present computational study, HF method gave higher values of the HOMO-LUMO energy gap and chemical hardness than B3LYP method. Similar values of other molecular properties are obtained in both the methods. The molecule has very low values of $\mu$, ω indicating that the DDT-4 acts more as a nucleophile than an electrophile. The high values of the HOMO-LUMO energy gap and chemical hardness indicate good aromatic character. This is probably due to the presence of two benzene rings and one thiazolidinedione ring in the molecule. Considering the values of $\mu$, ω, and η, it can be inferred that it acts as a nucleophile in its drug activity. The aromatic carbon atoms are rich as evidenced by the electronic distribution in the molecule and this may be the active site of drug action.

### *3.8 UV–vis spectra analysis*

Ultraviolet spectra analyses of PGZE have been studied by experimental and theoretical calculation values are shown in Table 7. Experimental electronic spectra measured in water, methanol, and ethanol solutions are presented in Figure.4. Three bands are observed in the electronic spectra of PGZE in all the solvents used in the studies. These absorptions are due to π-π* and n- π* transitions. The $\lambda_{max}$ at a short wavelength is due to π-π* transition and those at longer wavelengths are due to n- π* transitions. It is to be pointed out that there is a bathochromic shift in both the computed and experimental absorptions as we go from less polar solvent to more polar solvent. However, in methanol and ethanol solvents the computed $\lambda_{max}$ values for the three bands are greater than observed $\lambda_{max}$ values. While the agreement between the calculated and experimental λmax values of PGZE is evident, the calculated bands are blue-shifted by ~9 and ~2 nm.

**Table 7: Computed electronic spectral data of PGZE (wavelength of maximum absorption, λ (nm), excitation energies E (eV) and oscillator strengths (f) (a.u) using TD-DFT/B3LYP/6-311++G (d,p) method along with observed $\lambda_{max}$ values in different solvents**

| Solvent | Obs. $\lambda_{max}$ | λ (nm) | ΔE(eV) | *f* (a.u.) |
|---|---|---|---|---|
| Methanol | 276.00 | 302.52 | 4.09 | 0.0044 |
| | 242.00 | 265.39 | 4.67 | 0.0047 |
| | 224.00 | 261.62 | 4.73 | 0.0088 |
| Ethanol | 326.00 | 302.64 | 4.09 | 0.0045 |
| | 252.00 | 265.47 | 4.67 | 0.0047 |
| | 236.00 | 261.80 | 4.73 | 0.0065 |
| Water | 260.00 | 319.79 | 3.87 | 0.0164 |
| | 240.00 | 300.79 | 4.12 | 0.0070 |

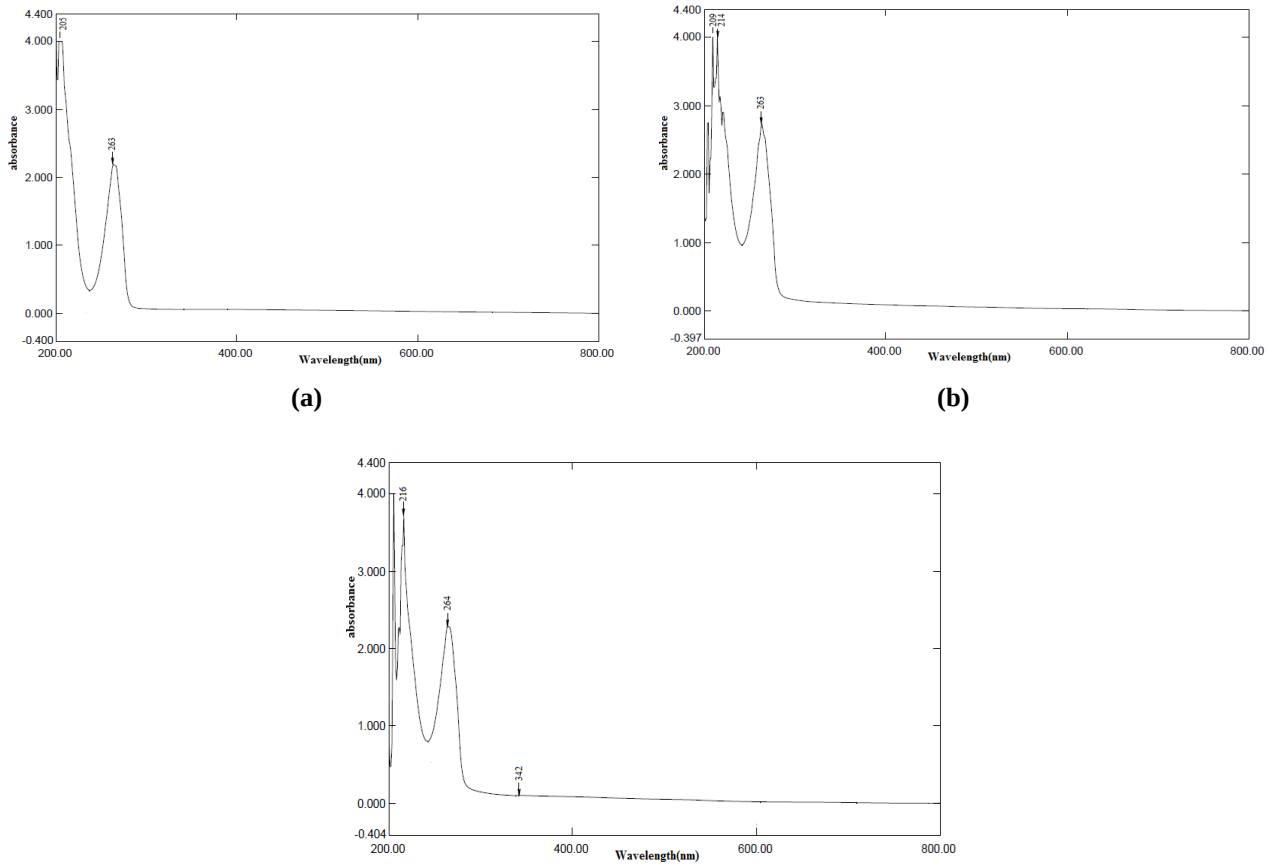


**(a)** **(b)**

**(c)**

**Fig.4. Experimental UV spectra of PGZE in (a) ethanol (b) methanol and (c) water**

## *3.9 Thermodynamic Properties*

The basis of vibrational analyses and statistical thermodynamics, the standard thermodynamic functions: such as self- consistent field (SCF) energy, zero-point vibrational energies (ZPVE), thermal energies, molar capacities at constant volume, enthalpy, entropy and dipole moment of molecule are calculated at 298K by the HF and B3LYP method using 6-311++G(d,p) as basis set and these computed values are listed in Table 8. It is found that the total energy obtained in HF and B3LYP methods are comparable. With regard to other thermodynamic properties, HF method yielded higher values than those obtained by the B3LYP method. The highest value of ZPVE is 243.24 kcal $mol^{-1}$ obtained in HF/6-311++G(d,p) method. These standard thermodynamic functions for the title molecule were calculated using Perl script THERMO.PL[44]. All the thermodynamic data supply helpful information for the further studies. These values can be used to compute the changes in thermodynamic properties and estimate the feasibility of chemical reactions using the second law of thermodynamics in thermo chemical field[45,46]. It must be remembered that all the thermodynamic functions were calculated for in gas phase.

**Table 8: Computed total energies (a.u.), zero point vibrational energy (kJ mol$^{-1}$), thermal energy (kJ mol$^{-1}$), molar heat capacity (J mol$^{-1}$ K$^{-1}$) ($C^{o}_{p,m}$), standard molar entropy (J K$^{-1}$ mol$^{-1}$) ($S^{o}_{m}$), standard Gibbs free energy (kJ mol$^{-1}$) ($G^{o}_{m}$) and standard enthalpy ($H^{o}_{m}$) (kJ mol$^{-1}$) of PGZE.**

| Parameters | HF/6-311++G(d,p) | B3LYP/6-311++G(d,p) |
|---|---|---|
| SCF energy | −1461.93 | −1461.74 |
| Zero-Point Vibrational Energy | 243.24 | 229.24 |
| Thermal Energy | 1075.28 | 1001.85 |
| Molar capacity at constant volume | 337.02 | 289.74 |
| Entropy | 714.33 | 548.85 |
| Gibbs free energy | 864.57 | 840.42 |
| Enthalpy | 1077.76 | 1004.25 |

## 4. CONCLUSIONS

In this study, we have used the HF and DFT/B3LYP methods to investigate theoretical analysis on the geometries and electronic properties of *Actos*, a new generation of non-steroidal anti-diabetes drug (NSAID), which act mainly by the inhibition of isoenzyme. The geometry was optimized and bond lengths and bond angles were obtained by HF and DFT methods. It may be pointed out that the bond lengths obtained by both HF and B3LYP methods are comparable and the bond lengths obtained by the B3LYP method are slightly longer than those calculated by HF method. The distortion in the symmetry of the ring due to the substitution of nitro group atom was discussed. The comparison between the experimental spectra (FT-IR, Raman) and calculated vibrational frequencies are the support of each other.NBO analysis is used to assess the intra-molecular delocalization in the molecule. It revealed that interaction energy in this molecule is due to the donor from LP(1)S1 to the BD*(1) C4-C5 which leads to the strongest stabilization of 240.7kJ/mol. The electronic distribution, in conjunction with electrophilicity index (ω) of indicates that the drug functions as a nucleophile and aromatic ring systems present in the molecule are the sites of its function as a DPP-4 inhibitor. The molecule has very low values of $\mu$, ω indicating that acts more as a nucleophile than an electrophile. Relatively low values of HOMO-LUMO energy gap and chemical hardness indicate significant aromatic character. The standard thermodynamic functions: such as self- consistent field (SCF) energy, zero-point vibrational energies (ZPVE), thermal energies, molar capacities at constant volume, entropy, enthalpy and dipole moment of molecule are calculated at 298K by HF and B3LYP method using 6-311++G(d,p) as basis set which can be used to compute the changes in thermodynamic properties and estimate feasibility of chemical reactions using second law of thermodynamics.

## REFERENCE

1. Forst A.P.T, Pioglitazone: an antidiabetic drug with the potency to reduce cardiovascular mortality.Expert Opin Pharmacother, 2006;7(4): 463-76.

2. Hirakata M , Tozawa R, Imura Y, Sugiyama Y. Comparison of the effects of pioglitazone and rosiglitazone on macrophage forum cell formation. Biochem Biophys Res Communication, 2005; 327(3): 967-8.
3. Sweetman SC, editors. *In:* Martindale: The complete drug reference, 33rd ed. Vol. I, USA: Pharmaceutical Press; 2002; 353.
4. Zhog WZ, Williams ME. Simultaneous quantitation of pioglitazone and its metabolites in human serum by liquid chromatography and solidphase extraction. J Pharm Biomed Ana 1996; 14: 465-73.
5. Yamashita K, Muarakami H, Okuda T, Motohashi M. High-performance liquid chromatographic determination of pioglitazone and its metabolites in human serum and urine. J Chrom 1996; 677:141-6.
6. Frisch M.J, et al., Gaussian 09, Revision B 04, Gaussian Inc., Pittsburg, PA, 2003.
7. Becke A.D, Density-functional thermochemistry. III. The role of exact exchange, J. Chem. Phys. 1993; 98: 5648-5652.
8. Lee C, Yang W, Parr R.G., LYP Gradient-corrected functional, Phys. Rev. B,1993; 37: 5648-5652.
9. Frisch A, Neilson A.B, Holder A.J, GAUSSVIEW, User Manual, Gaussian Inc., Pittsburgh, CT, 2009.
10. Keresztury G, Holly S, Verga Besenyei G, Wang A.Y, Durig J.R, Vibrational spectra of monothiocarbamates-II. IR and Raman spectra, vibrational assignment, conformational analysis and ab initiocalculations of S-methyl-N,N-dimethylthiocarbamate, Spectrochim. Acta, Part A ,1993; 49: 2007–2026.
11. Keresztury G, Chalmers J.M, Griffiths P.R, Raman Spectroscopy: Theory in Handbook of Vibrational Spectroscopy, John Wiley & Sons, London, 2002; 1:171–87.
12. Vayner E, Ball D.W, The energetic of the interaction of nitric oxide with alkali metal atoms, J. Mol. Struct. (Theochem), 2001; 542: 149-165.
13. Grete Gundersen, David W.H.Rankin, Molecular Structure of Bis (dimethylsilyl) amine in the gas-phase determined by electron-diffraction, Acta Chem. Scand. A, 1984; 38: 647–652.
14. Pulay P, Fogarasi G, Pongor G, Boggs J.E, Vargha A, J. Am. Chem. Soc. 1983; 10: 570-37.
15. Wang Y, Saebo S, Pittman C.U. Jr., J. Mol. Struct.: (Theochem.) 1993; 28: 9l-98.
16. Kalsi P.S, Spectroscopy of organic compounds. edn. VI, New Age International (P) Limited, New Delhi, 2005.
17. Vien D.L, Colthup N.B, Fateley W.G, Grasselli J.G, Handbook of Infrared and Raman Characteristic Frequencies of Organic Molecules, Academic Press,Boston. 1991.

18. Roeges N.P.G, A Guide to the Complete Interpretation of Infrared Spectra of Organic Structures, Wiley, New York. 1994.
19. Bellamy L.J, The Infrared Spectra of Complex Molecule, edn.III,Wiley, New York, 1975.
20. Silverstein M, Basseler G.C, Morill C, Spectrometric Identification of Organic Compounds, Wiley, New York, 1981.
21. Rastogi V.K , Palafox M.A , Tanwar R.P , Mittal L, Ab-initio calculations, FT-IR and FT-Raman spectra of 2-chloro-6-methyl benzonitrile, Indian Journal of Pure and Applied Physics 2010;48(2):85-94
22. Balachandran V, Santhi G, Karpagam V, Spectroscopic (FT-IR and FT-Raman) studies, NBO, HOMO–LUMO, NMR analyses and thermodynamics functions of 5-bromo-2-methoxybenzaldehyde. Spectrochim Acta Part A ,2013; 106: 262–274.
23. Altun A, Golcuk K, Kumru M, Theoretical and Experimental Studies of Vibrational Spectra of m-Methylaniline. J. Mol. Struct. (Theochem.) 2003; 625: 17-24.
24. Varsanyi G, Vibrational spectra of Seven Hundred Benzene Derivatives, Adam Hilger, London, 1974.
25. Bellamy L.J, Infrared Spectra of Complex Molecules.Wiley, New York, 1959.
26. Dollish F.R, Fateley W.G, Bentley F.F, Characteristic Raman Frequencies of Organic Compounds, John Wiley and Sons, New York, 1997.
27. Yang Y, Zhang W, Gao X, Blue-shifted and red-shifted hydrogen bonds: Theoretical study of the $CH_3CHO\cdots NH_3$ complexes, Journal of Molecular Structure: THEOCHEM. 2005; 732: 1-3 33-37.
28. R.S. Mulliken Electronic Population Analysis on LCAO–MO Molecular Wave Functions, J. Chem. Phys,1955; 23: 1833−1840.
29. Murray J.S, Sen K, Molecular Electrostatic Potentials, Concepts and Applications, Elsevier, Amsterdam, 1996.
30. Atalay Y, Avci D, Basoglu A, Linear and non-linear optical properties of some donor–acceptor oxadiazoles by ab initio Hartree-Fock calculations, Structural Chemistry,2008; 19: 239-246.
31. Fleming I, Frontier Orbitals, Organic Chemical Reactions, Wiley, London, 1976.
32. Parr R.G, Szentpaly L, Liu S, Electrophilicity index, J. Am. Chem. Soc. 1999; 121: 1922-1924.
33. Chattaraj P.K, Maiti B, Sarkar U, Electrophilicity equalization principle,J. Phys. Chem. 2003; 107A: 4973-4975.

34. Parr R.G, Donnelly R.A, Levy M, Palke W.E, Electronegativity: the density functional viewpoint, J. Chem. Phys. 1978; 68: 3801-3807.
35. R.G. Parr, R.G. Pearson, Absolute hardness: companion parameter to absolute electronegativity, J. Am. Chem. Soc. 1983; 105: 7512-7516.
36. R.G. Parr, P.K. Chattraj, Principle of maximum hardness, J. Am. Chem. Soc.,1991; 113: 1854-1855.
37. Parthasarathi R, Padmanabhan J, Elango M, Subramanian V, Chattaraj P, Variation of electrophilicity during molecular vibrations and internal rotations, Theoretical Chemistry Accounts, 2005; 113: 257–266.
38. Parthasarathi R, J. Padmanabhan, V. Subramanian, B. Maiti, P. Chattaraj, Toxicity analysis of 5- pentachlorobiphenyl through chemical reactivity and selectivity profiles, Curr. Sci. 2004; 86: 535-542.
39. Parthasarathi R, Padmanabhan J, Subramanian V, Sarkar U, Maiti B, Chattaraj P, Toxicity analysis of benzidine through chemical reactivity and selectivity profiles: a DFT approach, Int. Electron. J. Mol. Des, 2003; 2: 798-813.
40. Semire B, Semire B, Oyebamiji A, and M.Ahmad Theoretical Study on Structure and Electronic Properties of 2, 5Bis [4-N, N-Diethylaminostyryl] Thiophene and Its Furan and Pyrrole Derivatives Using DensityFunctional Theory (Dft) Pak. J. Chem., 2012; 2(4): 166-173.
41. B. Semire, O.A. Odunola, Theoretical study of the nucleophilic behavior of 3,4-dioxa-4-thia-cyclopenta[A]pentalene using ab initio and DFT based reactivity descriptors, Int. J. Chem. Model, 2011; 4: 87-96.
42. Domingo L.R, Aurell M.J, Perez P, Conteras P, Quantitative characterization of the local electrophilicity of organic molecules Understanding the regioselectivity on Diels-Alder Reactions, J. Phys. Chem. 2002; 106A: 6871-6875.
43. De Proft F, Geerlings P, Conceptual and computational DFT in the study of aromaticity, Chem. Rev. 2001; 101: 1451-1464.
44. Murray J.S, Sen K, Molecular Electrostatic Potentials, Concepts and Applications, Elsevier, Amsterdam, 1996.
45. R. Zhang, B. Dub, G. Sun, Y. Sun, Experimental and theoretical studies on *o*-, *m*- and *p*-chlorobenzylideneaminoantipyrines Spectrochim. Acta A, 2010; 75: 1115–1124.
46. E. Scrocco, J. Tomasi, in: P. Lowdin (Ed.), Advances in Quantum Chemistry,Academic Press, New York, 1978.